PROGRESS IN FAST IGNITOR RESEARCH WITH THE NOVA PETAWATT LASER FACILITY*

M. H. Key, E. M. Campbell, T. E. Cowan, B. A. Hammel, S. P. Hatchett, E. A. Henry
J. D. Kilkenny, J. A. Koch, A. B. Langdon, B. F. Lasinski, R. W. Lee, J. D. Moody
M. J. Moran, A. A. Offenberger**, D. M. Pennington, M. D. Perry, T. J. Phillips
T. C. Sangster, M S. Singh, R. Snavely, M. A. Stoyer, M. Tabak, M Tsukamoto***,
K. Wharton, S. C.Wilks.

Lawrence Livermore National Laboratory, P.O. Box 808, L-473
Livermore CA 94550 USA

ABSTRACT

The physics of fast ignition is being studied using a petawatt laser facility at the Lawrence Livermore National Laboratory. Performance of the PW laser with deformable mirror wavefront control giving intensities up to $3x10^{20}$ Wcm^{-2} is described. Measurements of the efficiency of conversion of laser energy to relativistic electrons and of their energy spectrum and angular distribution including an observed narrow beam angle of $\pm 15^{o}$, are reported. Heating by the electrons to near 1keV in solid density CD_2 is inferred from the thermo-nuclear neutron yield. Estimates suggest an optimized gain of 300x if the National Ignition Facility were to be adapted for fast ignition.

1. INTRODUCTION

The concept of the Fast Ignition (FI) [1] is of importance in inertial fusion energy (IFE) research because it offers the possibility of significantly higher gain than can be obtained in indirectly driven [2] or directly driven [3] inertially confined fusion (ICF). Higher gain would allow power generation with lower driver efficiency and FI is therefore attractive for laser driven IFE. Figure [1] illustrates this by showing the calculated gain for ICF targets of a size appropriate to the 1.8 MJ National Ignition Facility (NIF) which will start operation in the USA in 2002. The NIF target designs for indirect drive have been developed over decades of research and there is a sound basis for the predicted gain factor of 12 to 20. The research base for direct drive with predicted gains at NIF scale of 20 to 70 is less mature, but is nevertheless substantial. The potential for gain of about 300 indicated for FI at NIF scale is based on newer physics of the interaction of intense laser radiation with plasma in the relativistic regime and its practical feasibility remains to be proven.

---

*Work performed under the auspices of the U.S. Department of Energy by the Lawrence Livermore National Laboratory under Contract No. W-7405-ENG-48.

**Visiting from Department of Electrical Engineering, University of Alberta, Edmonton, Alberta, T6G 2G7, Canada

***Visiting from Joining & Welding Research Institute, Osaka University, Ibaraki, Osaka 567, Japan

The essential idea of fast ignition is to pre-compress the fusion fuel by conventional laser driven methods, then to ignite the fuel with a separate short duration high intensity laser pulse. A pre-cursor hole boring pulse creates a channel in the plasma atmosphere enabling the ignitor pulse to penetrate close to the dense fuel. Absorption of the ignitor pulse at the critical density interface generates a beam of relativistic electrons which transport energy to the dense fuel and heat the ignition spark. It must reach a temperature kT>10 keV over a density radius product ρr>0.5 gcm^{-2}[4] The mean energy of the electrons must be such that their energy is deposited within the spark and about 1MeV is therefore required. This paper discusses experimental work aimed at testing ideas relevant to FI using a laser beam line of up to 1 petawatt (PW) power at the Nova facility [5].

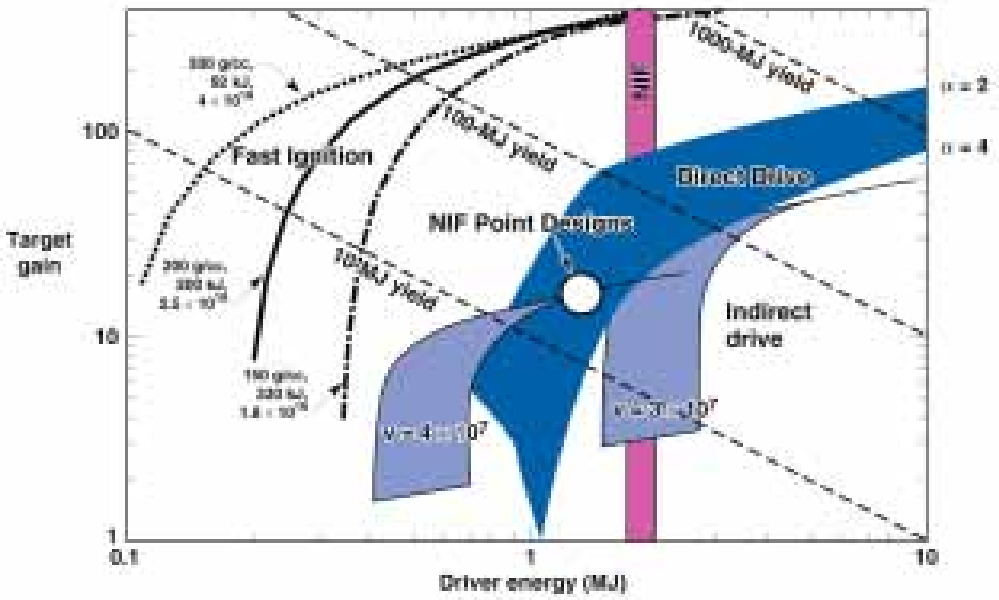

*FIG. 1. Calculated gain curves for laser driven ICF target*s. Fast *ignition plots are labeled with density, ignition spark driver energy and focal spot* $I\lambda^2$ *which are discussed in section 10*

2. THE PETAWATT LASER

Powerful short pulse lasers have become available through chirped pulse amplification (CPA) in high energy neodymium glass lasers and one beam line of the 10 beam Nova laser using disc amplifiers of up to 31.5 cm diameter, has been adapted with CPA to generate 0.8 kilojoule stretched pulses. Petawatt power is obtained when the stretched pulse is re-compressed via a pair of 1 meter diameter reflection gratings to a minimum duration of less than 500 ps [5]. The focal spot determines the intensity and a diffraction limited airy pattern would ideally be produced. In practice, the wave front quality is typically many times diffraction limited due both to passive optical imperfections and to thermal effects from heating of the laser glass by the flashlamps. The introduction of a computer controlled deformable mirror (DM) in the PW laser beam line at Nova has significantly improved the wavefront as illustrated in figure 2. A typical image without the DM after a 7 hour cooling delay, shows significant thermal distortions. The much improved focal spot shown with use of the DM is reproducible for firing intervals as short as 1 1/2 hours. Analysis of the ccd images allows determination of the spectrum of intensity. Typically, peak intensities reach values up to 3 $x10^{20}$ Wcm^{-2} for f/3 focussing when the laser is operated at a power of 1 PW and 20% of the energy is delivered above 10^{20} Wcm^{-2}. The fraction of the power contained up to the first minimum around the central focal spot is 30%. The Strehl ratio is 5% and the fwhm of the central focal spot is 2.5 times the diffraction limit.

There is laser energy incident on the target prior to the arrival of the short-pulse due to amplified spontaneous emission (ASE) and small fractional leakage of the short-pulse through Pockels cell gates in the pulse generator system. ASE begins approximately 4 ns prior to the short pulse at a roughly constant intensity and its energy is typically 3 x10^{-4} of the main pulse energy. A leakage pulse arrives 2 ns before the main pulse and its minimized energy is 10^{-4} of the main pulse. The ASE and leakage pre-pulse create a plasma from solid targets prior to the arrival of the main pulse and interaction of the main pulse with this plasma particularly by relativistic self focusing, is important in the conversion of laser energy to electron energy. Short-pulse optical interferometry has been used to measure the density structure of the pre-pulse induced plasma and these results have been compared with numerical simulations in 2 dimensional cylindrical symmetry using the hydrodynamic code Lasnex [6]. Good consistency of measured and computed results has allowed more routine determination of variations in the structure of the performed plasma from Lasnex modeling in conjunction with monitoring the ASE and prepulse levels on each shot.

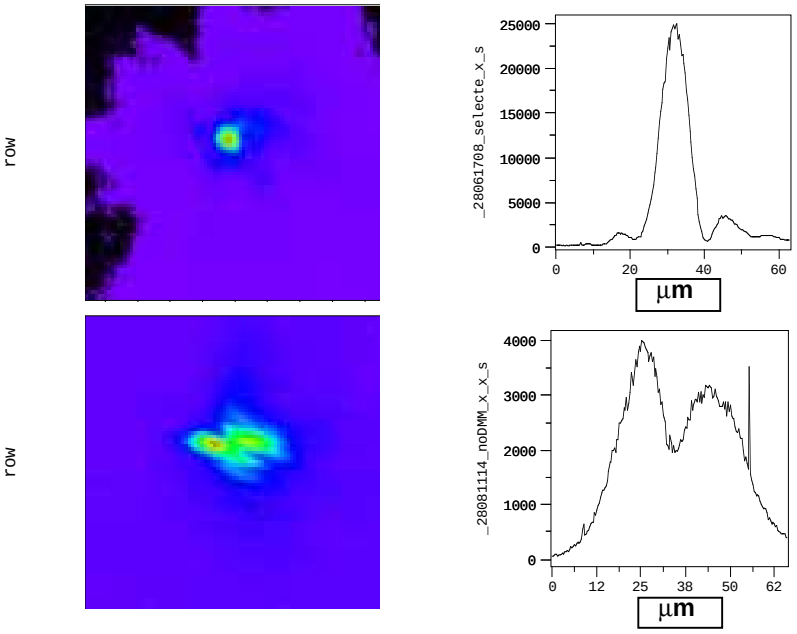

FIG. 2. Equivalent plane focal spot images and horizontal lineouts with (above) and without (below) the DM. The f.w.h.m. of the focal spot with the deformable mirror is 8 μm.

3. CONVERSION EFFICIENCY AND ENERGY SPECTRUM OF THE ELECTRONS

Conversion of up to 30% of the incident laser energy into electrons of mean energy exceeding 600 keV has been inferred from measurements the Kα fluorescence of a buried layer of Mo in Cu targets [7]. These measurements made at peak focused intensity of 2x10^{19} Wcm^{-2} in 0.5 ps pulses were obtained with 15 J laser pulses using a smaller scale prototype of the PW beam. The good efficiency and suitable mean energy of the electrons for application to fast ignition provide a basis for more detailed studies of the electron source.

The full scale PW system operating in both 0.5 ps and 5 ps pulses has been used to study the electron energy spectrum at peak intensities of 3x10^{20} and 3x10^{19} Wcm $^{-2}$ respectively. A magnetic electron spectrometer [8] was used to measure the energy spectra of the electrons. The targets in these

experiments were also used to produce high energy x-rays by bremsstrahlung and were typically 0.5 mm thick Au. Electrons emitted from the rear of these targets have therefore lost energy by both collisions and due to the electrostatic potential in the target. In spite of these losses; the recorded electron spectra have energies up to 100 MeV as shown in figure 3. The quasi-exponential slope of the electron energy spectrum can be used to estimate an equivalent temperature for the electron source and measurements in the region of above 10 MeV show apparent temperatures for both the 0.5 ps and 5 ps data of the order of 5 to 10 MeV. It is clear from these data that the tail has a higher temperature than would be inferred by assuming the temperature to be close to the ponderomotive potential at the vacuum intensity. Such an estimate gives 1 MeV and 3 MeV respectively for the long and short pulse data. The spectra were recorded at 30° from the laser direction and also at 95° for targets at normal incidence. It is evident from figure 3 that in the region around 10 MeV the electron flux is significantly larger in the forward direction. Interesting also is the observation of positrons produced by pair production in the Au target.

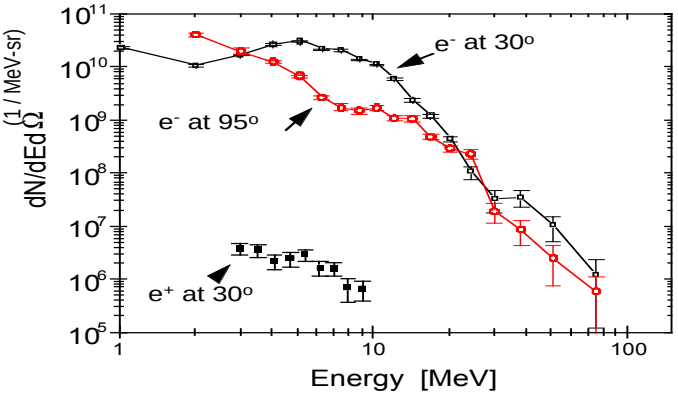

FIG. 3. Electron energy spectrum for a 280J, 0.5 ps pulse normally incident on a 0.5 mm thick Au target.

4. ANGULAR DISTRIBUTION OF X-RAY EMISSION

X-ray bremsstrahlung from relativistic electrons has a cone angle of $1/\gamma$ where γ is the relativistic factor. Consequently, measurements of the angular distribution of the x-ray emission at photon energies in the MeV region are almost equivalent to direct measurement of the angular distribution of the electron flux in the target. An array of 97 thermo-luminescent (TLD) detectors filtered to respond to photon energies greater than 300 keV, covered a ±45° cone of angles around the laser direction and was used to produce the map of x-ray emission shown in figure 4. The striking feature of these data is the broad angular range and multiple off axis peaks. Comparison of nominally identical shots shows that the pattern of these peaks changes randomly from shot to shot.

5. NUCLEAR ACTIVATION

High energy x-ray photons interacting with high z target materials induce photo-neutron emission and nuclear activation through nuclear giant resonance (γ,*xn*) processes. The resonances are relatively narrow and peak at energies which increase systematically with the number of ejected neutrons *x*. For example in Au, the peaks for *x=1* and *x= 7* are at about 15 MeV and 70 MeV. The product nuclei are typically in excited states whose γ emission can be measured and in our measurements using Au the yields for x=1,3,4,5,6 and 7 have been recorded. From the yields and known cross sections of these processes the absolute spectral intensity in the 15 to 70 MeV spectral

region covered by the peaks of these cross sections has been deduced. Figure [4] illustrates the angular distribution of the x-rays at high photon energy obtained from *x=1* nuclear activation of an Au disc composed of multiple smaller disks. The pattern has a typically broad off axis peak and there is evidence in figure [4] of splitting of the peak. The direction of the peak varies randomly. The TLD recorded patterns of 1MeV photons and the 15 MeV activation patterns have been seen to be uncorrelated.

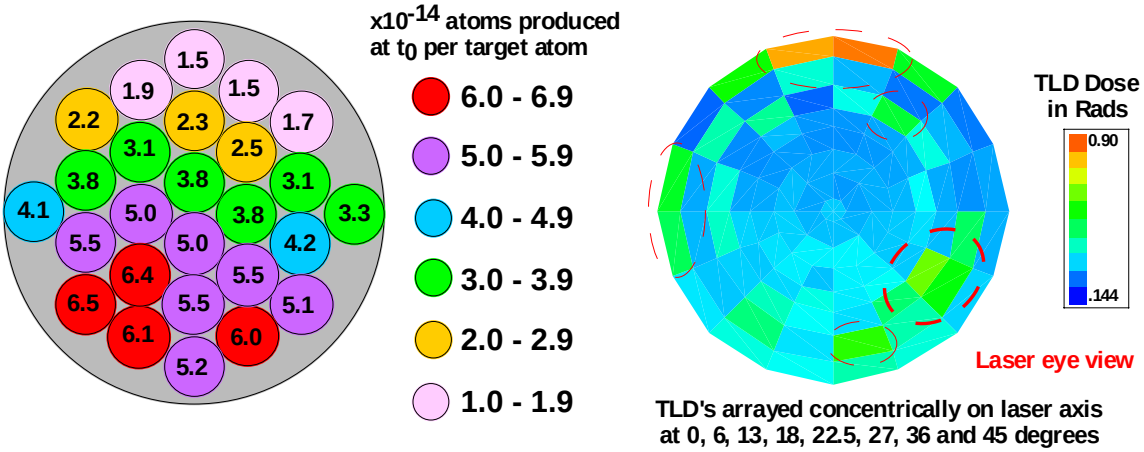

FIG. 4 Right; the angular pattern of x-ray emission recorded with a TLD array. Dashed lines ring the regions of higher intensity. Each segment represents one TLD. Left - Nuclear activation from 1 mm thick Au targets backed with 2 mm Ni and 1mm Au, the latter subdivided into 1 mm cylinders to map the angular pattern of activation over a range of $\pm 45^{o}$.

6. RELATIVISTIC CHANNELING

Evidence of relativistic channel formation is shown in figure 5. The laser was focused at variable distances in front of and behind the surface of a planar Au target at normal incidence and 550 J in 0.5 ps. The irradiated area on the target if the propagation of the laser were unaffected by the performed plasma, is shown by the superimposed circles. For focusing 300 μm in front of the target the x-ray pinhole camera images of the front surface of the target filtered to record x-rays of about 5 keV energy, shows an emission zone which is approximately 20 μm in diameter and much smaller than the nominal 100 micron diameter irradiated area. The image has structure suggesting one strong filament and 2 subsidiary filaments. Displacement of the target to the plane of best focus shows an essentially invariant x-ray image. When the laser was focused 200 μm behind the surface, the x-ray image was diffuse and of weak intensity extending over more than 300 μm diameter. It has one 10 μm diameter bright spot attributable to a small fraction of the beam undergoing relativistic self focusing. The yield of photo-neutrons was invariant at 2 to 3 $x10^{8}$ for focusing in front of the target while focusing behind the target surface gave a drop in yield to 10^{7}.

7. MECHANISMS INFLUENCING THE ELECTRON SOURCE

Possible causes for the stochastic behavior and wide beam divergence of x-ray emission include a hosing instability of the relativistic filament at near critical density, which has been seen in particle in cell (PIC) modeling [9] or Weibel instability breaking up the relativistic electron current into multiple off axis filaments which has also been seen in PIC modeling [10]. Refraction and multiple filamentation in the structure of preformed plasma may also contribute. The hot tail in the

energy spectrum of the electrons is attributable with some confidence to acceleration processes at sub-critical density which have recently been noted in PIC modeling to give apparent temperatures of more than 3 times the ponderomotive potential [11].

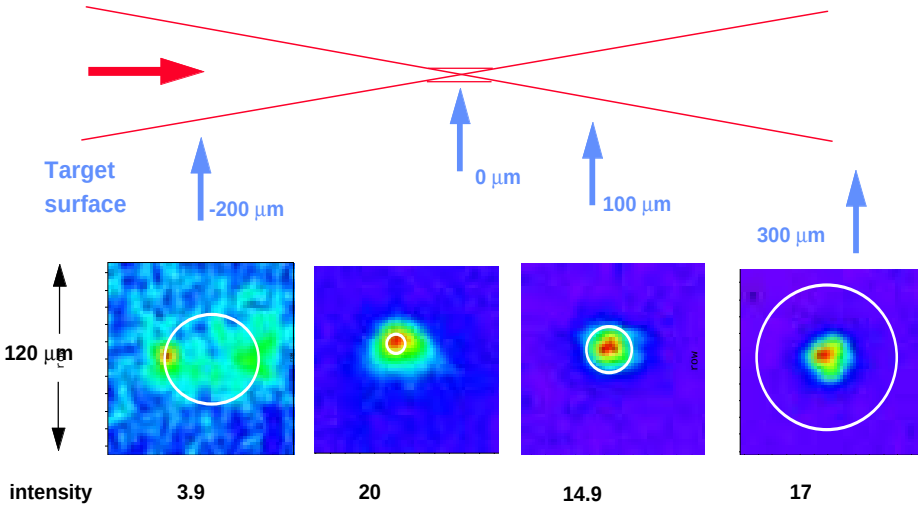

FIG. 5. X-ray pinhole camera images. The location of the target surface relative to the focal plane is indicated in the sketch.

8. ELECTRON EMISSION FOR P POLARIZED OBLIQUE INCIDENCE

In very recent experiments the angular distribution of electron emission has been measured for P polarized 45 degree incidence on CH polymer targets typically 100 μm thick using 5 ps laser pulses at energies up to 650 J. Here the absorption mechanism is different from the jxB process at normal incidence which creates two electron bursts per optical cycle. P polarized obliquely incident absorption is by the Brunel mechanism [12] in which electrons are driven perpendicular to the target surface from sub to super-critical density by the electric field of the laser. The absorption launches electrons into the target with the oscillation energy along the perpendicular to the target surface. The electrons were detected by a cone of radio-chromic film placed behind the target and centered on the laser axis. This film was in two layers, the first behind 7 μm of Al and the second layer behind an additional 200 μm of Ta. The first layer detected electrons with energies > 100 keV and the second > 500 keV. The image from the first layer showed the emission pattern in figure 6. An intense electron beam saturating the film is observed approximately normal to the target surface. Also of interest are weaker emission features, in particular, a line of emission (in a V shape on the unfolded cone of film) which corresponds to electrons accelerated in the plane of incidence over a $\pm 90^{o}$ range of angles relative to the laser beam. The second layer shows only the beam directed along the normal to the target surface. A line out of the optical density of the film indicates that the angular range of the beam is only $\pm 15^{o}$at full width half maximum of the optical density (which is approximately proportional to intensity). There is also interesting fine structure within the beam with an angular range of just a few degrees. This narrow well directed beam is extremely promising and interesting for application to fast ignition.

9. HEATING BY THE ELECTRONS

Theoretical work [13] has suggested that a beamed source of electrons in solid density material can be transported with magnetic collimation by its self-generated magnetic field. More

recent calculations [14] for intensity of 2 x 10^{19} Wcm^{-2} in a 15 μm focal spot show collimated heat flow with temperature reaching 3 keV on axis and 1keV out to a radius of 15 μm penetrating through 0.1mm of solid CD_2. This kind of heat transport is highly desirable for fast ignition.

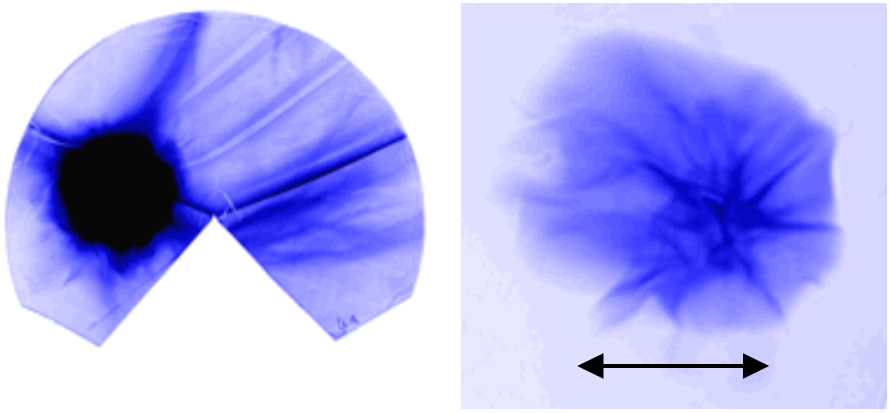

FIG Electron emission . Left- >100keV, pattern over forward hemisphere (original cone of film on a flat plane). Right- >500keV, enlarged view of beamed emission, (scale arrow shows 30^o range).

Moreover, the electron jet previously described is suitable to initiate this behavior. Targets of solid CD_2 with a surface layer of CH were irradiated with 5 ps pulses to study thermonuclear fusion reactions in the heated CD_2 which generate neutrons from DD fusion with an energy of 2.45 MeV and an energy spread in keV of 82(kT/1keV) $^{1/2}$. Such nearly mono-energetic thermal neutron emission is very different from the photo-neutron emission discussed earlier or neutron generation by accelerated deuterons striking static deuterons [15], both of which produce neutron energy spectra that are many MeV wide. Figure 7 shows a neutron spectrum recorded by a large aperture neutron scintillator array (Lansa) comprised of 960 photo-multiplier/scintillator detectors located 21.5 m from the target at an angle that is backward at 70^0 from the laser axis. The target had 10 μm CH over 100 μm CD_2 and was irradiated at 5 ps with 180J. The striking feature of the spectrum is a narrow peak at 2.45 MeV which is well above the noise level and cannot be attributed to statistical fluctuations. This peak implies emission of 6 x 10^4 thermo-nuclear neutrons and the yield (scaling as T^5) suggests heating to a temperature approaching 1 keV.

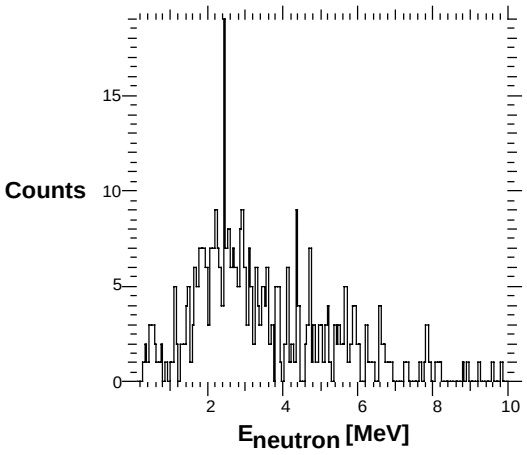

FIG 7 Lansa neutron energy spectrum showing a narrow peak of thermal DD fusion superimposed on a broad background

10. FAST IGNITION AT THE SCALE OF THE NIF

The energy required in the electron beam heating the ingnition spark has been determined from numerical simulations [16] and can be written in the form $80(100/\rho)^{1.8}$ kJ. The same analysis shows that the required density radius product ρr is 0.5 g cm^{-2}. Reducing the density therefore increases both the spark radius and its inertial confinement time. Larger radius and longer pulse reduce the required intensity at the laser focal spot. The electrons should have an energy deposition range equal to the spark ρr. A limit of about 1MeV is therefore imposed on the energy. The laser intensity x (wavelength)^2 or $I\lambda^2$ is consequently limited to approximately $2.5\text{x}10^{19}\text{Wcm}^{-2}\mu\text{m}^2$. At the scale of NIF these ignition requirements could be met with 10% of the NIF beams (i.e.19) focused in a clustered array of 25 μm diameter spots at 20 ps pulse duration and 0.53 μm wavelength, delivering 200 kJ. It is assumed here that hole boring brings the ignitor beams to within about 100 μm of the dense core, that there is 30% conversion to electrons and 66% efficient magnetically collimated transport with two fold increase in electron beam diameter to the ignition spark. Compression of the fuel is assumed to be with 8% hydrodynamic efficiency typical of direct drive and with a ratio α of internal energy to the Fermi degenerate minimum of 2. If 1 MJ of laser energy is used to compress the fuel, the mass is 4.1 mg with a diameter of 340 μm. the ρr is 3.4 gcm^{-2} and the burn efficiency given by ρr/(ρr+7), is 0.33. The gain i.e. ratio of burn yield to laser energy, is therefore 330. It is necessary for obtaining high gain that the total laser drive be well above the ignition threshold and this sets a lower limit on the density as illustrated in figure 1. The upper density limit arises from $I\lambda^2$ in the focal spots which increases with density as indicated in figure 1. In this scenario there is a narrow operating window at about 200 g/cc. The higher gain obtained in fast ignition arises because we assume high compression efficiency η=8%, a low adiabat ratio α=2 and a low density ρ=200 where the energy used to compress the fuel dominates the total input energy and scales as $\eta\alpha\rho^{2/3}$. Lower values of both α and ρ relative to direct drive are the source of the 5 to 10 fold higher gain for FI shown in figure 1. This simple model has many limitations. The requirement in fast ignition research is to substantiate that the postulated behaviors can be obtained. It is apparent that if they can be obtained then fast ignition has a unique capability for high gain of considerable potential importance for IFE.

[1] M. Tabak, J. Hammer, M.E. Glinsky, W.L. Kruer, S. C. Wilks, J. Woodworth, E. M. Campbell, M. D. Perry, Phys Plasmas, 1, 1626, (1994)
[2] J. D. Lindl, Laser Interaction and Related Plasma Phenomena, AIP Conf. Proc. 318, p. 635, (1993).
[3] S. E. Bodner, D. G. Colombant, J. H. Gardner, R. H. Lehmberg, S. P. Obenschain, L. Phillips, A.J. Schmitt, J. D. Sethian, R. L. McRory, W. Seka, C.P. Verdon, J. P. Knauer, B. B. Afeyan, H. T. Powell, Phys. Plasmas, 5,1901 (1998)
[4] S. Atzeni Jpn. J. Appl. Phys. 34 1980 (1995)
[5] M. D. Perry. Science and technology review. Publ. Lawrence Livermore National Laboratory UCRL-52000-96-12,p3. (1996)
[6] G. B. Zimmermann and W. L. Kruer , Comments on Plasma Phys. and Contr. Fusion 11,51 (1975)
[7] K. L. Wharton, S. P. Hatchett, S. C. Wilks, M. H. Key, J. D. Moody, V. Yanovski, A. A. Offenberger, B. A. Hammel, M. D. Perry , C. Joshi. Phys. Rev..Lett. 81, 822, (1998)
[8] T. Cowan et al. Lasers and Particle beams (to be published)
[9] B. Lazinski, A. B. Langdon, S. P. Hatchett, M. H. Key, M. Tabak, Phys. Plasmas (to be published)
[10] J. C. Adam et al. Proc. 3rd Int. Workshop on Fast Ignition. Publ. Rutherford Appleton Lab. (1998)
[11] S. C. Wilks et al. and also A. Pukhov and J. Meyer ter Vehn. Proc. 3rd Int. Workshop on Fast Ignition, Publ. Rutherford Appleton Lab. (1998)
[12] F. Brunel, Phys. Rev. Letts.. 59, 52 (1987)
[13] J. R. Davies, A. R. Bell, M. G. Haines, S. Guerin, Phys. Rev. E 56, 7193, (1997)
[14] J. Davies et al, Proc. 3rd Int. Workshop on Fast Ignition. Publ. Rutherford Appleton Lab. (1998)
[15] R. Kodama et al. Proc. 17th IAEA Fusion Energy Conference. Publ. IAEA Vienna. (1998)
[16] S. Atzeni Proc. 2nd Int. Workshop on Fast Ignition Publ. Max Planck Inst. fur Quanten Optik (1997)